Biochemistry
Article
pubs.acs.org/biochemistry

Structure of the Forkhead Domain of FOXA2 Bound to a Complete DNA Consensus Site

Jun Li,[†,‡] Ana Carolina Dantas Machado,[§,∥] Ming Guo,[†] Jared M. Sagendorf,[§,∥] Zhan Zhou,[†] Longying Jiang,[†] Xiaojuan Chen,[†,‡] Daichao Wu,[†] Lingzhi Qu,[†] Zhuchu Chen,[†] Lin Chen,[*,†,§] Remo Rohs,[*,§,∥] and Yongheng Chen[*,†,‡,⊥]

[†]Key Laboratory of Cancer Proteomics of Chinese Ministry of Health and Laboratory of Structural Biology, Xiangya Hospital, Central South University, Changsha, Hunan 410008, China

[‡]State Key Laboratory of Medical Genetics and College of Life Science, Central South University, Changsha, Hunan 410008, China

[§]Molecular and Computational Biology Program, Department of Biological Sciences and Department of Chemistry, University of Southern California, Los Angeles, California 90089, United States

[∥]Department of Physics and Astronomy and Department of Computer Science, University of Southern California, Los Angeles, California 90089, United States

[⊥]Collaborative Innovation Center for Cancer Medicine, Guangzhou, Guangdong 510060, China

Supporting Information

ABSTRACT: FOXA2, a member of the forkhead family of transcription factors, plays essential roles in liver development and bile acid homeostasis. In this study, we report a 2.8 Å co-crystal structure of the FOXA2 DNA-binding domain (FOXA2-DBD) bound to a DNA duplex containing a forkhead consensus binding site (GTAAACA). The FOXA2-DBD adopts the canonical winged-helix fold, with helix H3 and wing 1 regions mainly mediating the DNA recognition. Although the wing 2 region was not defined in the structure, isothermal titration calorimetry assays suggested that this region was required for optimal DNA binding. Structure comparison with the FOXA3-DBD bound to DNA revealed more major groove contacts and fewer minor groove contacts in the FOXA2 structure than in the FOXA3 structure. Structure comparison with the FOXO1-DBD bound to DNA showed that different forkhead proteins could induce different DNA conformations upon binding to identical DNA sequences. Our findings provide the structural basis for FOXA2 protein binding to a consensus forkhead site and elucidate how members of the forkhead protein family bind different DNA sites.

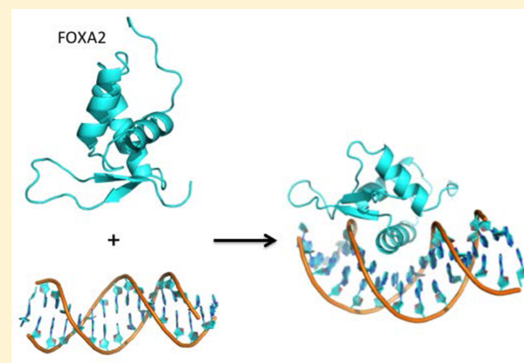

Forkhead box (FOX) proteins comprise a large family of transcription factors (TFs), members of which display functional diversity and participate in cellular processes ranging from development to immunity and metabolism.[1,2] More than 170 FOX family members have been identified from different species and classified into 19 subfamilies (from FOXA to FOXS).[3,4] FOXA, also known as hepatocyte nuclear factor 3 (HNF3), was initially discovered as a key transcriptional regulator in the liver and many endoderm-derived tissues.[5] Members of the FOXA subfamily can remodel nucleosomes and, as pioneer factors, facilitate DNA binding of other TFs.[6] In mammals, the FOXA subfamily consists of FOXA1 (HNF3α), FOXA2 (HNF3β), and FOXA3 (HNF3γ). FOXA2 is a master regulator of gene expression in the liver, participating in liver-specific gene transcription and related physiological activities.[7] This protein is essential for hepatic bile acid homeostasis and prevention of cholestatic liver injury.[7−9] Recent evidence suggests the idea that FOXA2 can affect the proliferation and invasiveness of pancreatic cancer cells and act as a tumor suppressor gene in pancreatic cancer.[10]

FOX family proteins contain a relatively conserved DNA-binding domain (DBD), known as the winged-helix or forkhead domain. The DBD of FOX is typically composed of three parts: three α-helices at the N-terminus, a three-stranded β-sheet, and two less conserved winged loops at the C-terminus (wings 1 and 2). The main DNA recognition region is located on the third helix (H3), which binds DNA by inserting into the DNA major groove. The amino acid sequence of H3 exhibits a high degree of homology among all FOX family members. Most paralogous FOX proteins bind to the canonical DNA response element 5′-RYAAAYA-3′ (R = A or G, and Y = C or T).[11−13] Sequence divergence in the wing regions contributes to differences in DNA binding.[14,15] The wing regions carry basic amino acids, which

Received: March 8, 2017
Revised: June 11, 2017
Published: June 23, 2017

 © 2017 American Chemical Society
DOI: 10.1021/acs.biochem.7b00211
Biochemistry 2017, 56, 3745−3753

potentially recognize DNA structural features in the flanking regions of FOX-binding sites, as previously observed for other transcription factor families.[16−18] For forkhead proteins, a recent analysis of HT-SELEX data demonstrated that binding specificity predictions improve for models that augment nucleotide sequence with DNA shape features.[19] In protein binding microarray experiments, forkhead proteins were shown to have the ability to specifically bind to alternate distinct DNA motifs.[20] These findings merit structural studies that compare binding mechanisms of paralogous FOX transcription factors.

The human full-length FOXA2 protein contains two transcription activation domains and a forkhead domain (Figure S1A).[21] Its DBD displays a high degree of sequence homology (95%) to FOXA1 and FOXA3 (Figure S1B).[22] The co-crystal structure of a FOXA3/DNA complex was previously reported,[23] but the DNA used for crystallization contained a nonconsensus binding site. Genome-wide analysis of FOXA2-binding sites by ChIP-seq in human and mouse adult liver tissues suggested that FOXA2 binds to the consensus sequence (5′-GTAAACA-3′) of the FOX family.[24,25] In this study, we determined the co-crystal structure of the FOXA2-DBD bound to a 16 bp DNA containing a consensus site (5′-GTAAACA-3′). We compared our structure with previously determined FOXA3 and FOXO1 co-crystal structures and employed biochemical analyses to study binding of FOXA2 to different DNA sites.

■ MATERIALS AND METHODS

Protein Expression and Purification. The coding region of the human FOXA2-DBD (residues 157−258) was cloned in the pGEX-6P1 vector. All constructs were confirmed by DNA sequencing (GenScript, NanJing, China). Protein was expressed in *Escherichia coli* Rosetta BL21 (DE3) cells and induced with 0.5 mM isopropyl β-D-1-thiogalactopyranoside for 6 h at 297 K. Protein was purified by using glutathione-Sepharose (GE Healthcare) according to a standard protocol. The GST affinity tag was removed by PresScission cleavage overnight at 277 K. Protein was further purified by cation-exchange (Mono S 5/50GL, GE Healthcare) and size-exclusion chromatography (Superdex 75 10/300 GL, GE Healthcare). Peak fractions were collected and concentrated to ∼26 mg/mL. The final protein was stored in storage buffer [10 mM Hepes, 300 mM NaCl, 10 mM $MgCl_2$, and 0.5 mM TCEP (pH 7.5)] at 193 K.

Duplex DNA Preparation. All DNAs were purchased from GenScript and purified as described previously.[26] The DBE2 (Daf-16 family binding element 2) sequence contains strands 5′-TGCAAAATGTAAACAAGACT-3′ and 5′-AGTCTTGTTTACATTTTGCA-3′.[27] The TTR (transthyretin) sequence contains strands 5′-TTGACTAAGTCAATCA-3′ and 5′-TGATTGACTTAGTCAA-3′.[23]

Crystallization, Data Collection, and Structure Determination. The FOXA2/DNA complex was prepared by mixing purified FOXA2 protein and DNA at 1:1.2 molar ratio with a final protein concentration of 10 mg/mL. Crystals were initially screened with the Hampton Natrix Kit by sitting drop vapor diffusion at 291 K. Crystals were optimized by the hanging drop method at 291 K, by using a well solution of 80 mM $Mg(OAc)_2$, 50 mM MES buffer, and 16−20% PEG 4K (pH 6.5). Crystals were stabilized in harvest/cryoprotectant buffer containing 80 mM $Mg(OAc)_2$, 50 mM MES buffer, 30% PEG 4K, and 20% glycerol (pH 6.5) and flash-frozen with liquid nitrogen for cryo-crystallography. Data were collected at the Shanghai Synchrotron Radiation Facility (SSRF) and BL17U1 beamline.

The co-crystal structure was determined as described previously.[28] Molecular replacement was performed using Phaser from the PHENIX package.[29] A previously determined FOXA3 structure [Protein Data Bank (PDB) entry 1VTN, chain C] was used as initial search model in the molecular replacement. The structure was further refined by using PHENIX. Statistical results of the crystallographic analysis are listed in Table 1. Figures were generated by PyMol.[30] DNAproDB was used to generate schematic diagrams of protein−nucleic acid interactions.[31]

Table 1. Data Collection and Refinement Statistics for the FOXA2-DBD/DNA Complex

resolution range (Å)	33.64−2.796 (2.896−2.796)
space group	C121
unit cell (*a*, *b*, *c*, α, β, γ)	195.126 Å, 71.932 Å, 72.155 Å, 90.0°, 103.14°, 90.0°
total no. of reflections	178752 (17848)
no. of unique reflections	23535 (2364)
multiplicity	7.5 (7.5)
completeness (%)	96.80 (86.05)
mean $I/\sigma(I)$	18.52 (2.71)
Wilson *B* factor	68.73
R_{merge}	0.1666 (3.753)
R_{meas}	0.1789
R_{work}	0.2298 (0.3499)
R_{free}	0.2811 (0.3964)
no. of non-hydrogen atoms	5425
macromolecules	5384
water	41
protein residues	460
RMSD for bonds (Å)	0.005
RMSD for angles (deg)	1.05
Ramachandran favored (%)	91
Ramachandran outliers (%)	3.4
Clashscore	10.38
average *B* factor	69.40
macromolecules	69.50
solvent	58.70

Isothermal Titration Calorimetry (ITC) Assays. ITC measurements were taken at 298 K on a NANO ITC instrument (TA Instruments). Duplex DNA and purified protein were dialyzed overnight in storage buffer [25 mM Hepes, 300 mM NaCl, 10 mM $MgCl_2$, and 1 mM TCEP (pH 7.0)]. Next, 50 μL of DNA at 100−200 μM was injected into a 15−20 μM FOXA2 protein solution (300 μL per sample cell). A 240 s interval between injections was used, to permit the signal to return to baseline before the next injection. Each injection volume was 2 μL. All data were analyzed by NANO Analysis software (TA Instruments). Heat generated by DNA dilution was used as a control. Standard free energies of binding and stoichiometry were obtained from the K_d and ΔH values derived from ITC curve fitting, respectively. To ensure the reliability of data, all experiments were repeated at least three times.

DNA Structure and Protein−DNA Interaction Analysis. Structures of DNA bound to FOXA2 (this study), FOXA3 (PDB entry 1VTN),[23] and FOXO1 (PDB entry 3CO7)[27] were analyzed with CURVES.[32] For comparison of these structures, we renamed the FOXA3 chains to align the structures and

DOI: 10.1021/acs.biochem.7b00211
Biochemistry 2017, 56, 3745−3753

perform binding site analysis in the same strand orientation. DNA structural features were compared between different binding sites. For visualization of protein–DNA interactions, contact maps were generated with the DNAproDB tool.[31] Labels were customized for the sake of simplicity. In certain cases, the recognition helix was renamed to "H3" for agreement with the standard forkhead nomenclature. To calculate the electrostatic potential in the DNA minor groove, DelPhi[33] was used to solve the nonlinear Poisson–Boltzmann equation as previously described.[34] To analyze the structure of unbound DNA targets, all-atom Monte Carlo (MC) simulations were performed by using a previously published method and protocol.[35,36] All possible hydrogen atom (H) positions were calculated for donor atoms (D) that satisfy specified geometrical criteria with acceptor atoms (A) in the vicinity. The following criteria were used: H–A distance of <2.7 Å, D–A distance of <3.35 Å, D–H–A angle of >90°, and H–A–AA angle of >90° (where AA is the atom attached to the acceptor). All possible hydrogen bonds were identified by finding all the prospective atoms that satisfy given geometric criteria between the hydrogen bond donors (D) and acceptors (A), and the D–A distance is <3.35 Å.[37]

PDB Entries. Atomic coordinates and structural factors of the FOXA2-DBD/DNA complex were deposited as RCSB Protein Data Bank entry 5X07.

■ RESULTS

Overall Structure of the FOXA2-DBD/DNA Complex. We determined the co-crystal structure of the FOXA2-DBD (residues 157–257) bound to a 16 bp double-stranded DNA containing a consensus binding element (5′-GTAAACA-3′) (Figure 1A). Co-crystals diffracted to a resolution of 2.8 Å and

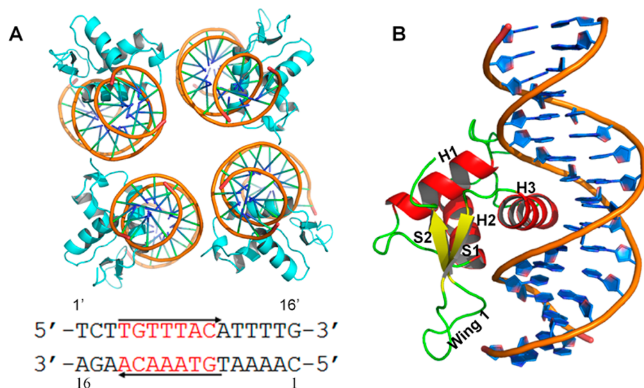

Figure 1. Co-crystal structures of the FOXA2-DBD/DBE2 complex. (A) Overall structure of the FOXA2 forkhead domain bound to the DBE2 element in an asymmetric unit. FOXA2 molecules are colored cyan, and DNA targets are colored orange. The sequence of the 16 bp DNA duplex (DBE2) used in the crystallization is also shown. (B) Structural representation of the FOXA2-DBD (chain C) bound to DBE2 DNA (chains A and B). Secondary structure elements are labeled.

belonged to space group *C*2 (Table 1). The asymmetric unit contained four FOXA2 forkhead domains and four double-stranded DNA segments. Each FOXA2 monomer adopted the canonical winged-helix fold[23,27] and comprised three α-helixes (H1–H3), two antiparallel β-strands (S1 and S2), and a loop (wing 1) between S1 and S2 (Figure 1B). Electron density was not observed for wing 2 of the FOXA2 forkhead domain, suggesting that this region might be flexible and disordered in the crystal. This finding was surprising because this region of FOXA2 is highly homologous to that of FOXA3, for which a previously published structure revealed the C-terminal region forming an extended loop (wing 2).

DNA Recognition by the FOXA2-DBD. DNA recognition by FOXA2 was dominated by H3, which inserted deeply into the major groove (Figure 2). Asn205 formed bidentate hydrogen bonds with Ade10, whereas His209 recognized Thy8′ and Ade9 with base-specific hydrogen bonds (Figure 2A,B). Arg202, Ser206, and Ser212 formed hydrogen bonds with the phosphate groups of Ade9, Thy8, and Thy7′, respectively (Figure 2A,B). Numerous van der Waals contacts also formed between FOXA2 and its corresponding DNA targets. In addition to helix H3, wing 1 of FOXA2 contributed to DNA binding. A pair of hydrogen bonds formed between the Gua5′ phosphate group and Ser231/Trp233. Lys219 interacted with the phosphate group of Thy6′ (Figure 2C).

Comparison of DNA Binding Affinity Using Isothermal Titration Calorimetry (ITC). In the previously determined FOXA3-DBD/DNA structure, the binding site of FOXA3 was 5′-GACTAAGTCAACC-3′, which is quite different from the consensus FOX-binding site (5′-GTAAACA-3′). We used ITC assays to compare the binding affinities of the FOXA2-DBD (same fragment as in the crystal structure determination) to different DNA target sites. Figure 3 shows representative binding isotherms and a detailed analysis of thermodynamic binding parameters. According to these results, the FOXA2-DBD bound to DNA with a 1:1 stoichiometric ratio. The K_d of the FOXA2 forkhead domain binding to the transthyretin (TTR) site was estimated to be ~1.5 μM. The K_d of FOXA2 binding to the Daf-16 family binding element 2 (DBE2) was estimated to be ~105 nM (Table 2). Thus, FOXA2 bound to the consensus site with a higher binding affinity.

In contrast to the previously reported FOXA3-DBD/TTR structure, the electron density of wing 2 (residues 240–258) in the FOXA2-DBD/DBE2 structure could not be observed. This result suggested that wing 2 was flexible and disordered in the crystal. To test whether wing 2 contributes to FOXA2-DBD/DNA binding, we constructed a truncated fragment of FOXA2 without wing 2 and measured the DNA binding ability using ITC. The binding affinity of FOXA2 was reduced by ~30-fold when the C-terminal wing 2 region was removed (Table 2). These results suggested that wing 2 of FOXA2 was important for optimal DNA binding.

Structural Comparison between FOXA2- and FOXA3-DBDs Bound to Dissimilar DNA Sequences. We sought to compare the properties of protein–DNA binding among FOXA subfamily members by superimposing the FOXA3-DBD/DBE2 structure with the previously reported FOXA3-DBD/TTR structure (PDB entry 1VTN).[23] Despite the high degree of sequence homology between FOXA2 and FOXA3 (Figure S1B), their structures differed when bound to different DNA targets (Figure 4A). In the previously reported structure, wing 2 was ordered, whereas it was flexible in the FOXA2-DBD/DBE2 structure (Figure 4A).

In addition to analyzing the overall structure, we compared the structures in terms of their protein–DNA interactions. Bidentate hydrogen bonds between Asn and Ade were conserved in both structures (Figure 4B). His209 in the FOXA2-DBD/DBE2 structure formed a hydrogen bond with Thy8′, whereas this hydrogen bond did not exist in the FOXA3-DBD/TTR structure because the corresponding nucleic acid was replaced with guanine (Figure 4C). Arg210 of FOXA3 (corresponding to Arg250 in FOXA2) formed hydrogen bonds with Thy4 and

DOI: 10.1021/acs.biochem.7b00211
Biochemistry 2017, 56, 3745–3753

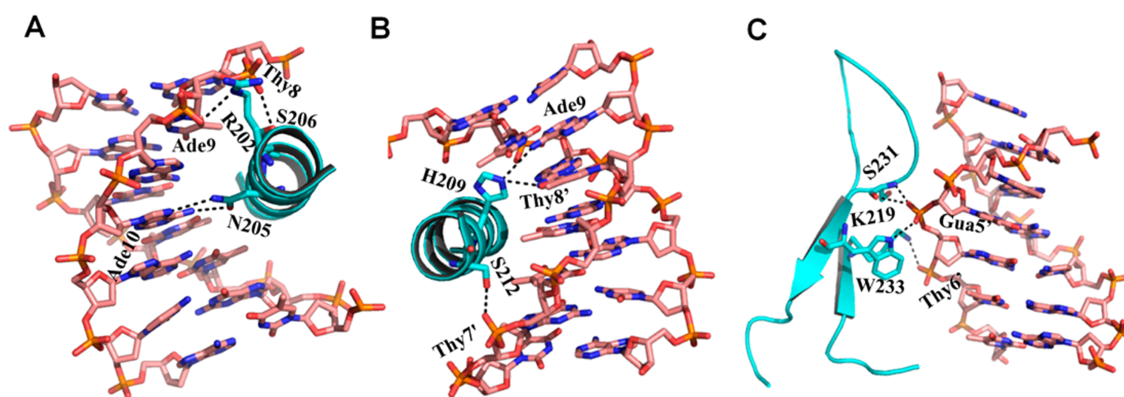

Figure 2. DNA recognition by the FOXA2 DBD domain. (A and B) Hydrogen bonds between helix 3 of FOXA2 and DNA. (C) Interactions between wing 1 and DNA.

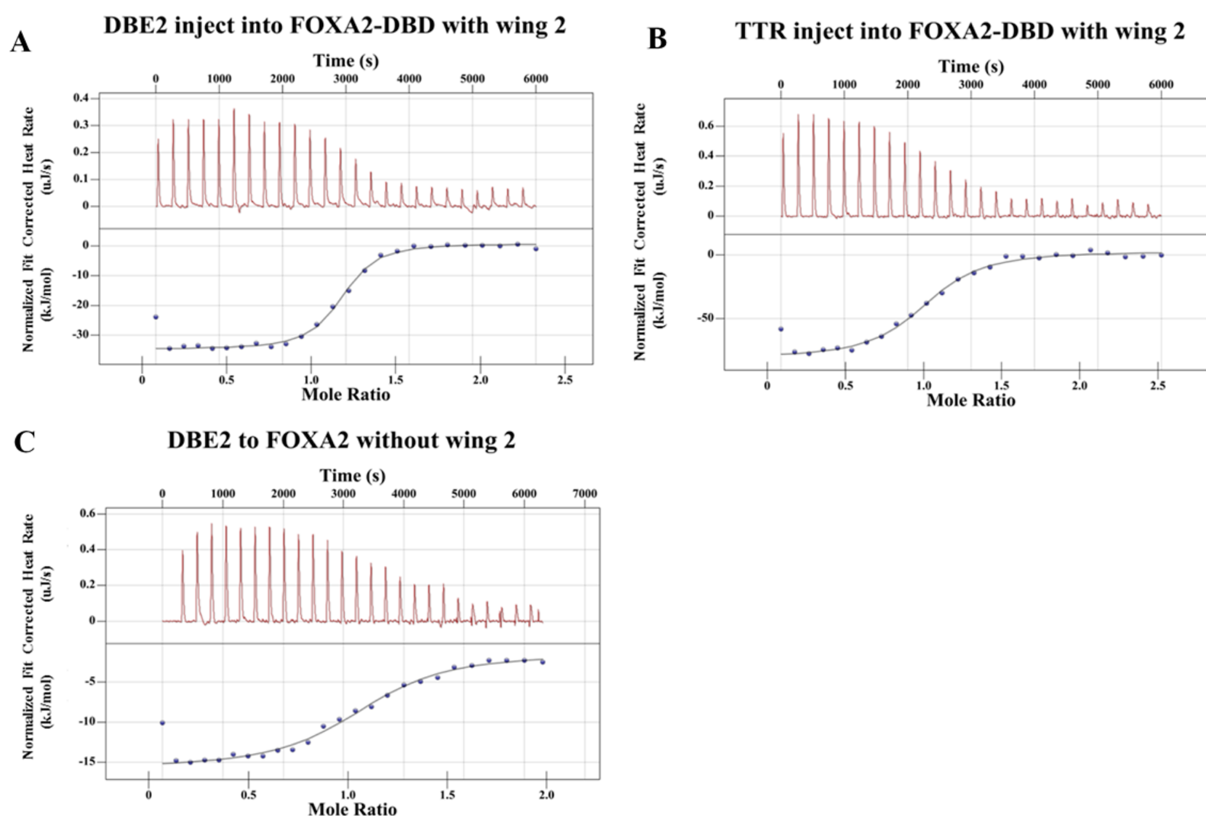

Figure 3. Binding affinity measurement of protein−DNA interactions by quantitative ITC. Quantification of the interaction between the FOXA2-DBD and DNA derived from different DNAs by ITC. Representative power−response curves (top) and heats of reaction normalized to the moles of protein injected (bottom).

Table 2. Thermodynamic Parameters of the Interaction[a]

protein	DNA	K_d (nM)	N	ΔH (kJ/mol)	ΔS (J mol^{-1} K^{-1})
FOXA2 (157−257)	TTR	1500 ± 200	1.0 ± 0.1	−12.26 ± 0.5	58.2 ± 0.8
FOXA2 (157−257)	DBE2	105 ± 20	1.2 ± 0.1	−35.54 ± 2	14 ± 5
FOXA2 (157−239)	DBE2	3500 ± 300	1.1 ± 0.1	−14.38 ± 0.6	55.8 ± 0.5

[a]All data were measured at 298 K in 25 mM Hepes (pH 7.5), 300 mM NaCl, 10 mM $MgCl_2$, and 1 mM TCEP buffer. Values represent at least three independent experiments corresponding to the average deviation.

Gua31, whereas these interactions were not observed in the FOXA2-DBD/DBE2 structure because this region was flexible in that structure (Figure 4D).

We also analyzed DNA structural features for the DBE2 DNA bound by the FOXA2-DBD. This analysis revealed a widening of the minor groove within the center of the core binding site, with a maximum located at the TpA step, followed by an adjacent narrowing (Figure 5A, cyan line) around the AT-rich flanking region. To differentiate between an intrinsic or induced shape, we performed all-atom MC simulations of the free DNA. This

DOI: 10.1021/acs.biochem.7b00211
Biochemistry 2017, 56, 3745−3753

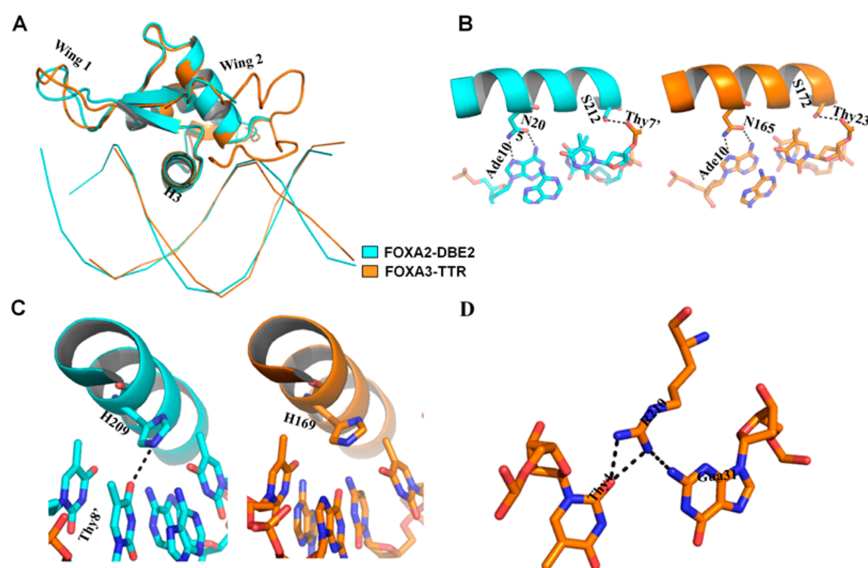

Figure 4. Comparison with a previously determined FOXA3-DBD/TTR structure (PDB entry 1VTN).[23] (A) Overall structural comparison between FOXA2 (cyan) and previous FOXA3 (orange). (B) Bidentate hydrogen bonds between Asn and Ade were conserved in both structures. (C) A hydrogen bond formed between His209 and Thy8′ in the FOXA2-DBD/DBE2 structure but not in the FOXA3-DBD/TTR structure. (D) FOXA3 Arg210 formed hydrogen bonds with DNA in the FOXA3-DBD/TTR structure.

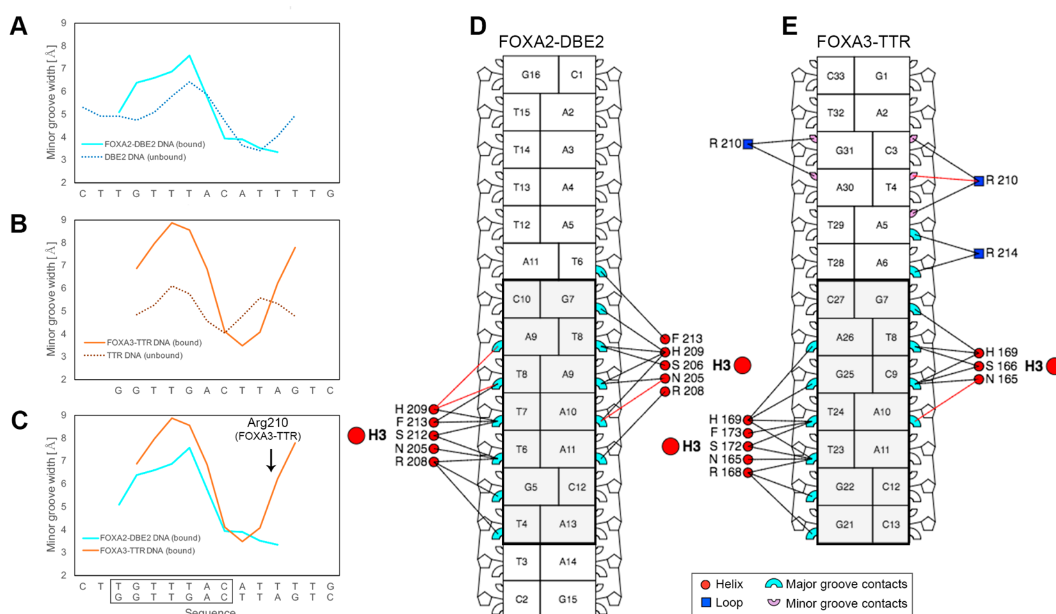

Figure 5. Structural analysis of FOXA2 and FOXA3 DNA-binding sites. (A−C) Minor groove widths of FOXA-bound and unbound DNAs, showing comparisons between (A) the FOXA2-bound DBE site and the unbound DBE2 site, (B) the FOXA3-bound TTR site and the unbound TTR site, and (C) FOXA2-bound DBE2 and FOXA3-bound TTR. (D and E) Schematic diagrams show interactions between the forkhead domain and the DNA major and minor groove in a nucleotide−residue interaction map for (D) FOXA2-DBD/DBE2 and (E) FOXA3-DBD/TTR complexes. Nucleotide−residue red and black lines represent interactions that involve hydrogen bonds and other contacts, respectively. Images were generated with DNAproDB.[31] Black rectangles (C−E) highlight the core binding element recognized by these FOXA proteins.

analysis revealed that the deformation pattern was intrinsic and already apparent in the shape of the unbound DNA target (Figure 5A, dotted blue line).

Next, we investigated whether the DNA structural features of FOXA-binding sites could be important for DNA shape readout.[38] In the case of FOX proteins, besides the major groove recognition, wings 1 and 2 could a play role in shape readout at the edges and flanking regions of the core binding site. In addition to our current FOXA2-DBD/DBE2 complex, we also analyzed the DNA structure of the previously published FOXA3-DBD/TTR complex because of its protein similarity and well-defined electron density of wing 2.[23]

The DNA target site in the FOXA3-DBD/DNA complex (TTR) adjusted to protein binding in a similar manner as the target bound by FOXA2 (DBE2) (Figure 5A,B), despite differences in the sequences of their core DNA-binding sites. Comparing the FOXA3-bound to the FOXA2-bound target, we found that the minor groove width of the FOXA3-DBD/TTR complex followed the same pattern as that of the FOXA2-DBD/DBE2 complex, with an increased maximum (by ∼1.3 Å) for the

DOI: 10.1021/acs.biochem.7b00211
Biochemistry 2017, 56, 3745−3753

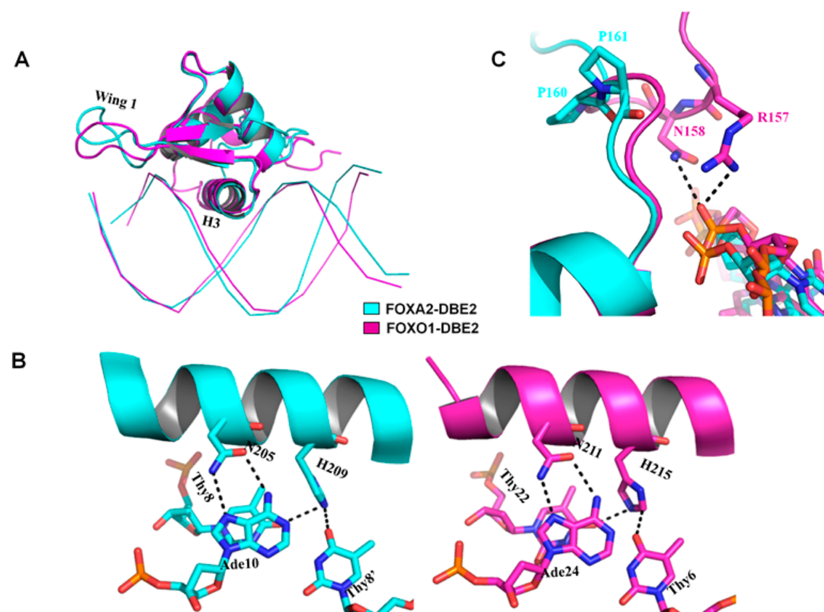

Figure 6. Comparison with the previously determined FOXO1-DBD/DBE2 structure (PDB entry 3CO7). (A) Overall structural comparison between FOXA2-DBD/DBE2 (cyan) and FOXO1-DBD/DBE2 (magenta) complexes. (B) Most hydrogen bonding interactions were conserved between the structures. (C) Structural comparison shows that the N-terminal tail of the FOXO1-DBD is located closer to the minor groove, although the protein is bound to the same DNA. Arg157 and Asn158 of FOXO1 (magenta) interact with the DNA backbone. The presence of Pro160 and Pro161 of FOXA2 (cyan) orients the N-terminal tail of the FOXA2-DBD away from the minor groove.

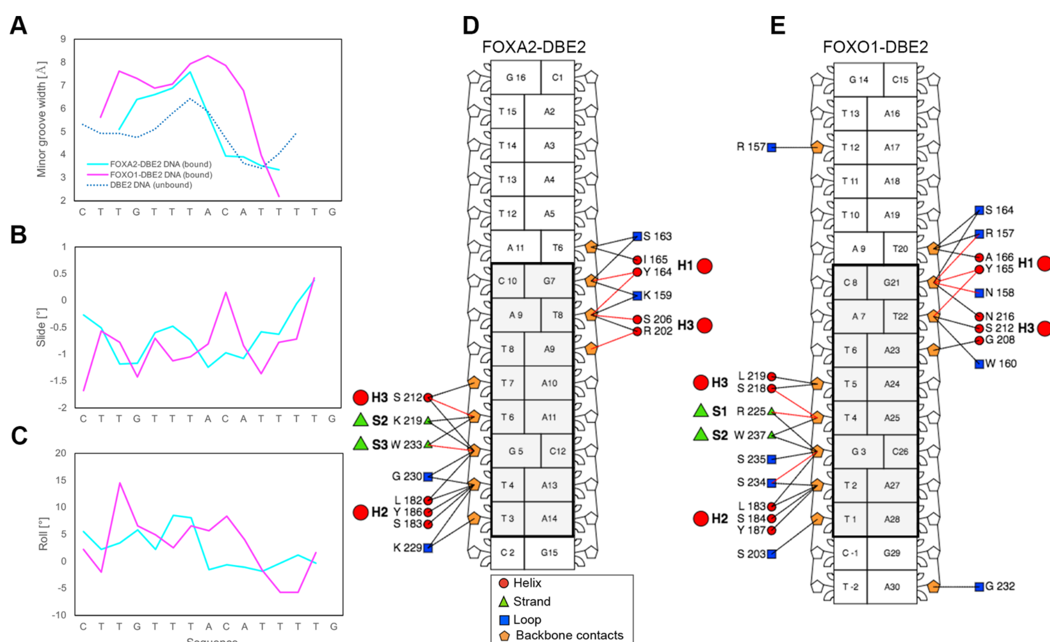

Figure 7. Structural analysis of DNA in complex with FOXA2 and FOXO1 DBDs. (A−C) Comparison of DNA shape features between FOXA2 and FOXO1 complexes, showing (A) minor groove widths of bound and unbound DNAs and (B and C) slide and roll angles for FOXA2 and FOXO1 DBE2 DNAs. Bound DBE2 is colored cyan (FOXA2) and magenta (FOXO1), while unbound DBE2 is shown as a dotted blue line. (D and E) Schematic diagram showing interactions between the forkhead domain and the DNA backbone as a nucleotide−residue interaction map for (D) FOXA2-DBD/DBE2 and (E) FOXO1-DBD/DBE2 complexes. Backbone contacts display slight differences between FOXA2-DBD/DBE2 and FOXO1-DBD/DBE2 complexes. Nucleotide−residue contacts (red and black lines) represent interactions that involve hydrogen bonds and other contacts, respectively. Images were obtained using DNAproDB.[31] Black rectangles (D and E) highlight the core binding element in the DBE2 DNA site.

FOXA3-bound DNA and a similar minimum (Figure 5C). For the free DNA, maximal and minimal minor groove widths were comparable for the two sequences, although the maximum was shifted by one nucleotide position and the minimum by two positions (Figure 5A,B). For the FOXA3-DBD/TTR target site, the region of minor groove narrowing coincided with the location where Arg210 of wing 2 inserted into the minor groove. This is also a region of increased negative electrostatic potential (Figure S3), which would favor interaction of Arg210 with the DNA. Arg210 is not exactly located at the minor groove minimum; instead, it is closer to the A30/T4 base pair (Figure 5E), where it forms a hydrogen bond with Thy4. This

DOI: 10.1021/acs.biochem.7b00211
Biochemistry 2017, 56, 3745−3753

observation is consistent with an electrostatic potential-dependent recognition of narrow minor groove regions.[39]

DNAproDB analysis of the protein−DNA contacts of the complexes highlighted an intricate pattern of interactions (Figure 5D,E). The analysis indicated a greater number of contacts for the FOXA2-DBD in the major groove than for the FOXA3-DBD, whereas the latter showed contacts in the minor groove that were not observed in the FOXA2-DBD/DBE2 complex. Therefore, the well-defined electron density of FOXA3-DBD/TTR wing 2 might be a result of enhanced interactions between wing 2 and the minor groove, as a way to stabilize the complex due to the decreased number of contacts in the major groove.

Overall, we found that highly homologous FOXA2- and FOXA3-DBDs induce a deformation similar to that of their DNA target sites upon binding, in spite of their different DNA sequences. This is observed in a scenario in which the FOXA2-DBD displays an increased number of hydrogen bonds in the major groove when compared to the FOXA3-DBD, whereas the wing 2 region is disordered. These differences may contribute to binding affinity differences of the FOXA2 protein when it binds to different DNA target sites.

Structural Comparison between FOXA2- and FOXO1-DBDs Bound to Similar DNA Sequences. To study the structural variations induced upon binding of different FOX proteins to the same DNA sequence, we compared the DNA conformation of our FOXA2 complex to that of the previously published FOXO1,[31] both bound to DNA sequence DBE2 (Figure 6). The proteins shared similar overall structures, with slight differences in the wing 1 region and the N-terminal tail (Figure 6A). The major groove in the FOXA2-DBD/DBE2 structure was wider than in the FOXO1-DBD/DBE2 structure (Figure 6A). We also examined interactions between the proteins and their DNA target sites. In the structures, asparagine and histidine in the FOXA2 and FOXO1 proteins, respectively, formed the same interaction network with the corresponding bases (Figure 6B). A major difference in DNA binding lies at the N-terminal tail. The N-terminal tail of FOXO1 forms a closer contact to DNA, and Arg157 and Asn158 of FOXO1 interact directly with the DNA backbone (Figure 6C). The sequence differences in this region between two proteins may contribute to this difference. The N-terminal tail of FOXA2 has two prolines (Pro160 and Pro161), in contrast to the same region in FOXO1.

Despite the DNA-binding sequence being the same in both the FOXA2 and FOXO1 complexes, the minor groove width changes observed upon protein binding are strikingly different. In particular, the minor groove width changes on the DBE2 target DNA induced upon protein binding in both complexes (Figure 7A) deviated more from each other than the changes observed upon the binding of more similar FOXA proteins bound to different DNA-binding sites [FOXA2-DBD/DBE2 and FOXA3-DBD/TTR (Figure 5C)]. Compared to the FOXA2-bound DNA, the DNA bound by FOXO1 has its maximal minor groove width shifted by one nucleotide position and was more distorted at the edges of the core binding site (Figure 7A, magenta line). Furthermore, the minor groove width maximum was increased by ∼1.8 Å, and the minimum was decreased by ∼1.2 Å compared to the values of free DNA. These findings indicate a more distorted DNA when it is compared to the same sequence bound by the FOXA2-DBD (Figure 7A, cyan line). Other DNA shape parameters also varied as a result of accommodating these two different proteins (Figure 7C,D), particularly at the CpA step.

Although neither protein showed base-specific contacts with the minor groove, the N-terminal tail of FOXO1 was directed toward the minor groove, allowing for an increased number of closer contacts with the backbone compared to the number for FOXA2 (Figure 6C; in Figure 7D,E, loop residues make contacts with the backbone). This positioning could explain the widening of the minor groove observed in this region (Figures 6A and 7A). Furthermore, the wing 1 region differed between these two proteins, leading to slightly different contacts with the backbone of the flanking regions (Figure 7 and Figure S2).

■ DISCUSSION

FOXA2 plays important roles in the initiation of liver development and normal bile acid homeostasis.[8] In human and mouse adult liver tissues, ChIP-seq analysis showed that FOXA2 preferentially bound to the FOX consensus sequence 5′-RTAAAYA-3′ (R = A or G, and Y = C or T).[24,25] The FOXA3 protein could also bind to a nonconsensus DNA site.[23] It has, however, remained unclear how FOXA proteins recognize different DNA-binding sites. Hydroxyl radical footprinting and site-directed mutagenesis indicated that the wing regions, especially wing 1, are crucial for optimal DNA binding.[14] In this study, we determined the co-crystal structure of FOXA2 bound to a DNA consensus site. ITC data showed that FOXA2 bound to DBE2 with a binding affinity higher than its affinity for TTR. These observations suggest that the highly similar FOX proteins FOXA2 and FOXA3 may bind to different DNA targets through adaptations of their protein−DNA interactions.

Most forkhead proteins recognize a common binding site (RTAAAYA, where R = A or G and Y = C or T).[11] We observed that FOXA2 bound to a DAF-16 family binding element (5′-GTAAACAA-3′), which was also the recognition element of FOXO1. Although FOX proteins recognized the DNA binding element with remarkable similarity, their DNA binding specificities displayed marked variability. Each forkhead protein has its own nucleotide preference at the R and Y positions in the core motif and flanking regions.[11] For example, although DBE1 and DBE2 share a common core motif, FOXO1 exhibited a 5-fold higher binding affinity for DBE2 than for DBE1 because of the thymine-rich 3′ flanking sequence.[27] On the other hand, different FOX proteins could induce different DNA deformations (e.g., strong bending of the DNA helix[11]). Our study suggests that, upon binding of different FOX proteins, DNA can adapt through changes in shape parameters.

Wing regions might play important roles in the DNA binding of FOX proteins.[40,41] Nuclear magnetic resonance data revealed that wing 1 is disordered in the absence of DNA.[42,43] This region undergoes rearrangement upon DNA binding, binding to the minor groove through direct hydrogen bonds and van der Waals contacts.[42] Amino acid composition and length variations might contribute to DNA binding differences. Wing 1 in the FOXP subfamily is much shorter than wing 1 in the FOXA subfamily and makes limited DNA contacts. Therefore, the FOXP forkhead domain binds DNA with a binding affinity lower than that of FOXA.[44] Wing 1 might act as a cofactor recognition target. In the crystal structure of the FOXP2/NFAT/DNA ternary complex, wing 1 served as a primary interaction site of the two TFs.[45] Wing 2 is well-ordered upon DNA binding in some co-crystal structures but disordered in others. In the FOXA3-DBD/DNA structure, wing 2 formed an extended loop that bound DNA extensively; in the FOXP2-DBD/DNA and FOXM-DBD/DNA structures, wing 2 adopted an α-helical structure (H5).[44,46] Although wing 2 cannot be defined in the FOXO1-DBD/DNA

DOI: 10.1021/acs.biochem.7b00211
Biochemistry 2017, 56, 3745−3753

and FOXA2-DBD/DNA structures,[27] biochemical studies suggest that this region is important for optimal DNA binding.

The N-terminal tail of the forkhead domain might also contribute to DNA binding. Interestingly, for the DBE2 DNA-binding site, this region was shown to interact with the DNA backbone in the FOXO1 complex, but not in the FOXA2 complex. By investigating structural features of other forkhead structures, we found that the positioning of the N-terminal tail varies across other members of this family, showing interactions with the DNA backbone in FOXK2 and FOXM1 complexes, but not with that of FOXP3.[47] Sequence differences in the region among these proteins might contribute to the differences in DNA binding because this region is not conserved among forkhead transcription factors (Figure S1). In addition, DNA sequence also contributes to the binding differences. In the case of FOXO1, the N-terminal tail binds to DBE2 DNA,[27] but not to G6PC1 DNA.[48]

In summary, the structure of the FOXA2-DBD/DNA complex revealed the mechanism by which the FOXA2 forkhead domain binds to the consensus FOX-binding sequence (5′-GTAAACA-3′). ITC experiments showed that the FOXA2-DBD binds to the DBE2 consensus site with a binding affinity higher than its affinity for the TTR site. This result is consistent with our structural observations that the FOXA2-DBD formed more interactions with the DBE2 site than with the TTR site. In addition, structural comparison with the FOXO1-DBD/DBE2 complex showed that different forkhead proteins could induce different DNA deformations when binding to the same DNA target site.

■ ASSOCIATED CONTENT

Supporting Information

The Supporting Information is available free of charge on the ACS Publications website at DOI: 10.1021/acs.biochem.7b00211.

Three figures (PDF)

■ AUTHOR INFORMATION

Corresponding Authors

*E-mail: yonghenc@163.com.
*E-mail: rohs@usc.edu.
*E-mail: linchen@usc.edu.

ORCID

Remo Rohs: 0000-0003-1752-1884
Yongheng Chen: 0000-0001-8139-6892

Funding

This work was supported by the National Natural Science Foundation of China (Grants 81372904 and 81570537 to Y.C. and Grant 81272971 to Z.C.) and the National Institutes of Health (Grants U01GM103804 and R01GM106056 to R.R. and Grants R01AI113009 and R01GM064642 to L.C.). R.R. is an Alfred P. Sloan Research Fellow.

Notes

The authors declare no competing financial interest.

■ ACKNOWLEDGMENTS

The authors thank Minjiong Li from the staff of the Shanghai Synchrotron Radiation facility (SSRF) for help with data collection.

■ REFERENCES

(1) Hannenhalli, S., and Kaestner, K. H. (2009) The evolution of Fox genes and their role in development and disease. *Nat. Rev. Genet. 10* (4), 233−40.

(2) Lam, E. W., Brosens, J. J., Gomes, A. R., and Koo, C. Y. (2013) Forkhead box proteins: tuning forks for transcriptional harmony. *Nat. Rev. Cancer 13* (7), 482−95.

(3) Tuteja, G., and Kaestner, K. H. (2007) SnapShot: forkhead transcription factors I. *Cell 130* (6), 1160.e1.

(4) Tuteja, G., and Kaestner, K. H. (2007) Forkhead transcription factors II. *Cell 131* (1), 192.

(5) Friedman, J. R., and Kaestner, K. H. (2006) The Foxa family of transcription factors in development and metabolism. *Cell. Mol. Life Sci. 63* (19−20), 2317−28.

(6) Iwafuchi-Doi, M., Donahue, G., Kakumanu, A., Watts, J. A., Mahony, S., Pugh, B. F., Lee, D., Kaestner, K. H., and Zaret, K. S. (2016) The Pioneer Transcription Factor FoxA Maintains an Accessible Nucleosome Configuration at Enhancers for Tissue-Specific Gene Activation. *Mol. Cell 62* (1), 79−91.

(7) Bochkis, I. M., Schug, J., Rubins, N. E., Chopra, A. R., O'Malley, B. W., and Kaestner, K. H. (2009) Foxa2-dependent hepatic gene regulatory networks depend on physiological state. *Physiol. Genomics 38* (2), 186−95.

(8) Bochkis, I. M., Rubins, N. E., White, P., Furth, E. E., Friedman, J. R., and Kaestner, K. H. (2008) Hepatocyte-specific ablation of Foxa2 alters bile acid homeostasis and results in endoplasmic reticulum stress. *Nat. Med. 14* (8), 828−36.

(9) Gosalia, N., Yang, R., Kerschner, J. L., and Harris, A. (2015) FOXA2 regulates a network of genes involved in critical functions of human intestinal epithelial cells. *Physiol. Genomics 47* (7), 290−7.

(10) Vorvis, C., Hatziapostolou, M., Mahurkar-Joshi, S., Koutsioumpa, M., Williams, J., Donahue, T. R., Poultsides, G. A., Eibl, G., and Iliopoulos, D. (2016) Transcriptomic and CRISPR/Cas9 technologies reveal FOXA2 as a tumor suppressor gene in pancreatic cancer. *Am. J. Physiol. 310* (11), G1124−G1137.

(11) Pierrou, S., Hellqvist, M., Samuelsson, L., Enerbäck, S., and Carlsson, P. (1994) Cloning and characterization of seven human forkhead proteins: binding site specificity and DNA bending. *EMBO J. 13* (20), 5002−5012.

(12) Chen, X., Ji, Z., Webber, A., and Sharrocks, A. D. (2016) Genome-wide binding studies reveal DNA binding specificity mechanisms and functional interplay amongst Forkhead transcription factors. *Nucleic Acids Res. 44* (4), 1566−78.

(13) Koh, K. P., Sundrud, M. S., and Rao, A. (2009) Domain Requirements and Sequence Specificity of DNA Binding for the Forkhead Transcription Factor FOXP3. *PLoS One 4* (12), e8109.

(14) Cirillo, L. A., and Zaret, K. S. (2007) Specific interactions of the wing domains of FOXA1 transcription factor with DNA. *J. Mol. Biol. 366* (3), 720−724.

(15) Boura, E., Silhan, J., Herman, P., Vecer, J., Sulc, M., Teisinger, J., Obsilova, V., and Obsil, T. (2007) Both the N-terminal loop and wing W2 of the forkhead domain of transcription factor Foxo4 are important for DNA binding. *J. Biol. Chem. 282* (11), 8265−75.

(16) Schöne, S., Jurk, M., Helabad, M. B., Dror, I., Lebars, I., Kieffer, B., Imhof, P., Rohs, R., Vingron, M., Thomas-Chollier, M., and Meijsing, S. H. (2016) Sequences flanking the core-binding site modulate glucocorticoid receptor structure and activity. *Nat. Commun. 7*, 12621.

(17) Levo, M., Zalckvar, E., Sharon, E., Dantas Machado, A. C., Kalma, Y., Lotam-Pompan, M., Weinberger, A., Yakhini, Z., Rohs, R., and Segal, E. (2015) Unraveling determinants of transcription factor binding outside the core binding site. *Genome Res. 25* (7), 1018−1029.

(18) Dror, I., Zhou, T., Mandel-Gutfreund, Y., and Rohs, R. (2014) Covariation between homeodomain transcription factors and the shape of their DNA binding sites. *Nucleic Acids Res. 42* (1), 430−441.

(19) Yang, L., Orenstein, Y., Jolma, A., Yin, Y., Taipale, J., Shamir, R., and Rohs, R. (2017) Transcription factor family-specific DNA shape readout revealed by quantitative specificity models. *Mol. Syst. Biol. 13* (2), 910.

DOI: 10.1021/acs.biochem.7b00211
Biochemistry 2017, 56, 3745−3753

(20) Nakagawa, S., Gisselbrecht, S. S., Rogers, J. M., Hartl, D. L., and Bulyk, M. L. (2013) DNA-binding specificity changes in the evolution of forkhead transcription factors. *Proc. Natl. Acad. Sci. U. S. A. 110* (30), 12349−12354.
(21) Pani, L., Overdier, D. G., Porcella, A., Qian, X., Lai, E., and Costa, R. H. (1992) Hepatocyte nuclear factor 3 beta contains two transcriptional activation domains, one of which is novel and conserved with the Drosophila fork head protein. *Mol. Cell. Biol. 12* (9), 3723−3732.
(22) Lalmansingh, A. S., Karmakar, S., Jin, Y., and Nagaich, A. K. (2012) Multiple modes of chromatin remodeling by Forkhead box proteins. *Biochim. Biophys. Acta, Gene Regul. Mech. 1819* (7), 707−15.
(23) Clark, K. L., Halay, E. D., Lai, E., and Burley, S. K. (1993) Co-crystal structure of the HNF-3/fork head DNA-recognition motif resembles histone H5. *Nature 364* (6436), 412−420.
(24) Wederell, E. D., Bilenky, M., Cullum, R., Thiessen, N., Dagpinar, M., Delaney, A., Varhol, R., Zhao, Y., Zeng, T., Bernier, B., Ingham, M., Hirst, M., Robertson, G., Marra, M. A., Jones, S., and Hoodless, P. A. (2008) Global analysis of in vivo Foxa2-binding sites in mouse adult liver using massively parallel sequencing. *Nucleic Acids Res. 36* (14), 4549−64.
(25) Levitsky, V. G., Kulakovskiy, I. V., Ershov, N. I., Oshchepkov, D. Y., Makeev, V. J., Hodgman, T. C., and Merkulova, T. I. (2014) Application of experimentally verified transcription factor binding sites models for computational analysis of ChIP-Seq data. *BMC Genomics 15*, 80.
(26) Chen, Y., Bates, D. L., Dey, R., Chen, P. H., Machado, A. C., Laird-Offringa, I. A., Rohs, R., and Chen, L. (2012) DNA binding by GATA transcription factor suggests mechanisms of DNA looping and long-range gene regulation. *Cell Rep. 2* (5), 1197−206.
(27) Brent, M. M., Anand, R., and Marmorstein, R. (2008) Structural basis for DNA recognition by FoxO1 and its regulation by posttranslational modification. *Structure 16* (9), 1407−16.
(28) Wu, D., Guo, M., Philips, M. A., Qu, L., Jiang, L., Li, J., Chen, X., Chen, Z., Chen, L., and Chen, Y. (2016) Crystal Structure of the FGFR4/LY2874455 Complex Reveals Insights into the Pan-FGFR Selectivity of LY2874455. *PLoS One 11* (9), e0162491.
(29) Adams, P. D., Afonine, P. V., Bunkóczi, G., Chen, V. B., Echols, N., Headd, J. J., Hung, L.-W., Jain, S., Kapral, G. J., Grosse Kunstleve, R. W., McCoy, A. J., Moriarty, N. W., Oeffner, R. D., Read, R. J., Richardson, D. C., Richardson, J. S., Terwilliger, T. C., and Zwart, P. H. (2011) The Phenix software for automated determination of macromolecular structures. *Methods 55* (1), 94−106.
(30) Warren, L. D. (2004) *PyMOL User's Guide*, DeLano Scientific, San Carlos, CA.
(31) Sagendorf, J. M., Berman, H. M., and Rohs, R. (2017) DNAproDB: an interactive tool for structural analysis of DNA-protein complexes. *Nucleic Acids Res. 45* (W1), W89−W97.
(32) Lavery, R., and Sklenar, H. (1989) Defining the structure of irregular nucleic acids: conventions and principles. *J. Biomol. Struct. Dyn. 6* (4), 655−67.
(33) Honig, B., and Nicholls, A. (1995) Classical electrostatics in biology and chemistry. *Science 268* (5214), 1144−1149.
(34) Rohs, R., West, S. M., Sosinsky, A., Liu, P., Mann, R. S., and Honig, B. (2009) The role of DNA shape in protein-DNA recognition. *Nature 461* (7268), 1248−1253.
(35) Rohs, R., Sklenar, H., and Shakked, Z. (2005) Structural and energetic origins of sequence-specific DNA bending: Monte Carlo simulations of papillomavirus E2-DNA binding sites. *Structure 13* (10), 1499−509.
(36) Zhang, X., Dantas Machado, A. C., Ding, Y., Chen, Y., Lu, Y., Duan, Y., Tham, K. W., Chen, L., Rohs, R., and Qin, P. Z. (2014) Conformations of p53 response elements in solution deduced using site-directed spin labeling and Monte Carlo sampling. *Nucleic Acids Res. 42* (4), 2789−2797.
(37) McDonald, I. K., and Thornton, J. M. (1994) Satisfying Hydrogen Bonding Potential in Proteins. *J. Mol. Biol. 238* (5), 777−793.
(38) Rohs, R., Jin, X., West, S. M., Joshi, R., Honig, B., and Mann, R. S. (2010) Origins of specificity in protein-DNA recognition. *Annu. Rev. Biochem. 79*, 233−69.
(39) Harris, R., Mackoy, T., Dantas Machado, A. C., Xu, D., Rohs, R., and Fenley, M. O. Opposites attract: Shape and electrostatic complementarity in protein-DNA complexes. In *Innovations in Biomolecular Modeling and Simulation*; Schlick, T., Ed.; Royal Society of Chemistry: London, UK, 2012; Vol. 2, pp. 53−80.
(40) Overdier, D. G., Porcella, A., and Costa, R. H. (1994) The DNA-binding specificity of the hepatocyte nuclear factor 3/forkhead domain is influenced by amino-acid residues adjacent to the recognition helix. *Mol. Cell. Biol. 14* (4), 2755−2766.
(41) Marsden, I., Jin, C., and Liao, X. (1998) Structural changes in the region directly adjacent to the DNA-binding helix highlight a possible mechanism to explain the observed changes in the sequence-specific binding of winged helix proteins. *J. Mol. Biol. 278* (2), 293−9.
(42) Liu, P. P., Chen, Y. C., Li, C., Hsieh, Y. H., Chen, S. W., Chen, S. H., Jeng, W. Y., and Chuang, W. J. (2002) Solution structure of the DNA-binding domain of interleukin enhancer binding factor 1 (FOXK1a). *Proteins: Struct., Funct., Genet. 49* (4), 543−553.
(43) Jin, C., Marsden, I., Chen, X., and Liao, X. (1999) Dynamic DNA contacts observed in the NMR structure of winged helix protein-DNA complex. *J. Mol. Biol. 289* (4), 683−690.
(44) Stroud, J. C., Wu, Y., Bates, D. L., Han, A., Nowick, K., Paabo, S., Tong, H., and Chen, L. (2006) Structure of the forkhead domain of FOXP2 bound to DNA. *Structure 14* (1), 159−66.
(45) Wu, Y., Borde, M., Heissmeyer, V., Feuerer, M., Lapan, A. D., Stroud, J. C., Bates, D. L., Guo, L., Han, A., Ziegler, S. F., Mathis, D., Benoist, C., Chen, L., and Rao, A. (2006) FOXP3 controls regulatory T cell function through cooperation with NFAT. *Cell 126* (2), 375−87.
(46) Littler, D. R., Alvarez-Fernandez, M., Stein, A., Hibbert, R. G., Heidebrecht, T., Aloy, P., Medema, R. H., and Perrakis, A. (2010) Structure of the FoxM1 DNA-recognition domain bound to a promoter sequence. *Nucleic Acids Res. 38* (13), 4527−38.
(47) Chen, Y., Chen, C., Zhang, Z., Liu, C. C., Johnson, M. E., Espinoza, C. A., Edsall, L. E., Ren, B., Zhou, X. J., Grant, S. F. A., Wells, A. D., and Chen, L. (2015) DNA binding by FOXP3 domain-swapped dimer suggests mechanisms of long-range chromosomal interactions. *Nucleic Acids Res. 43* (2), 1268−1282.
(48) Singh, P., Han, E. H., Endrizzi, J. A., O'Brien, R. M., and Chi, Y.-I. (2017) Crystal structures reveal a new and novel FoxO1 binding site within the human glucose-6-phosphatase catalytic subunit 1 gene promoter. *J. Struct. Biol. 198* (1), 54−64.

DOI: 10.1021/acs.biochem.7b00211
Biochemistry 2017, 56, 3745−3753